JOURNAL OF CATALYSIS 145, 73–78 (1994)

Synthesis, Characterization, and Catalytic Properties of Metallo–Titanium Silicate Molecular Sieves with MEL Topology

J. Sudhakar Reddy,* Rajiv Kumar,*,[1] and Sigmund M. Csicsery†

*National Chemical Laboratory, Pune 411 008, India, and †Lafayette, California 94549

Received February 24, 1992; revised October 21, 1992

The synthesis and characterization of metallo–titanium silicate analogs (M = Al or Fe) with MEL structure are reported. The simultaneous incorporation of both M^{3+} (Al^{3+} or Fe^{3+}) and Ti^{4+} in the MEL framework provides dual catalytic properties in both oxidation (e.g., oxyfunctionalization of *n*-hexane) and acid catalyzed reactions (e.g., ethylbenzene disproportonation and *m*-xylene isomerization). The [*M*, Ti]–MEL molecular sieves, compared to the [*M*]–MEL analogs, were (i) more resistant towards deactivation in ethylbenzene disproportionation and *m*-xylene isomerization and (ii) less para selective in the latter reaction. © 1994 Academic Press, Inc.

INTRODUCTION

The framework substitution of Al^{3+} and/or Si^{4+} by other metal ions (such as Fe^{3+}, Ga^{3+}, Ge^{4+} etc.,) into the framework of various zeolites is one of the major developments in the area of molecular sieves (1–14). The isomorphous substitution of Si by Ti into MFI and MEL structures enlarged the application of these molecular sieves in the field of organic fine chemicals. The simultaneous incorporation of a trivalent metal ion (e.g., B^{3+}, Al^{3+}, Ga^{3+}, or Fe^{3+}) along with Ti^{4+} in MFI (15–18), MEL (19), and beta (20) structures has also been reported recently. It may be anticipated that such solids exhibit catalytic properties in both oxidation (due to Ti) and Brønsted acid (Al^{3+}, Fe^{3+}, and Ga^{3+}) catalyzed reactions. In this paper, we report the first detailed synthesis, characterization and catalytic properties of alumino–titanium silicate and ferri–titanium silicate molecular sieves with MEL topology. Their catalytic properties in both oxidation (oxyfunctionalization of *n*-hexane) and acid catalyzed reactions (*m*-xylene isomerization (21, 22) and ethylbenzene disproportionation (23, 24)) are reported.

[1] To whom correspondence should be addressed.

EXPERIMENTAL

Synthesis

The synthesis of metallo–titanium silicates was carried out from mixtures containing tetraethylorthosilicate (TEOS) (Fluka, 98%), tetrabutylorthotitanate (TBOT) (Fluka, 98%), tetrabutyl ammonium hydroxide (TBA-OH) (Aldrich), corresponding metal (III) nitrate solutions (aluminium nitrate and ferric nitrates, respectively) and water. Since the presence of alkali metal ions inhibits the incorporation of Ti into the framework (8, 12), no alkali metal salts were added. The following molar gel composition was used,

$$SiO_2/M_2O_3 = 90; \quad SiO_2/TiO_2 = 65;$$
$$SiO_2/(TBA)_2O = 10; \quad H_2O/SiO_2 = 30$$

where M = Al or Fe.

The synthesis procedures for [Al, Ti]–MEL and [Fe, Ti]–MEL are given below:

[Al, Ti]–MEL. A quantity of 54.9 g TBA–OH (20% aq. solution) was added to a solution of 45 g TEOS. This mixture was stirred for 20 min. A solution of 1.13 g TBOT in 10 g dry isopropyl alcohol was added to the above mixture slowly. To the above clear liquid, a solution of 1.77 g aluminium nitrate in 15 g water was added before the remaining 56 g water. The resultant mixture was stirred for 1 h and autoclaved at 443 ± 2 K for 2 days under static conditions.

[Fe, Ti]–MEL. A quantity of 45 g TEOS was slowly added to a solution containing 1.9 g ferric nitrate and 15 g water under stirring. After about 30 min. another solution of 1.13 g TBOT in 10 g dry isopropyl alcohol was added under vigorous stirring. Finally 54.9 TBA-OH

0021-9517/94 $5.00

(20% aq. Solution) in 56 g water was added. The resultant mixture was stirred for 1 h before autoclaving. The crystallization was carried out at 443 ± 1 K for 4 days under static conditions.

For the synthesis of [*M*]–MEL (*M* = Al or Fe) TBOT was not added. Similarly, Al or Fe was not used in the preparation of [Ti]–MEL (10–12). The crystalline material from the synthesis was filtered, washed, dried and calcined at 773 K first in dry N_2 for 8 h and then in air for an additional 10 h. For catalytic studies, the H-form of all the materials (prepared by ion-exchange twice with 1 *N* ammonium acetate) were calcined at 723 K for 8 h in flowing air and were used in the form of particles of 45–55 mesh size.

Characterization

Si, *M* (*M* = Al or Fe) contents were determined by ICP (John Yvon JYU-38 VHR) and Ti content was determined by XRF (Rigaku, 3070). The crystallinity of the products was determined by X-ray powder diffraction (Rigaku, MAX 3D) using the following equation:

$$\text{Crystallinity} = \frac{\text{Peak area between } 2\theta = 21.5\text{–}25.5^\circ \text{ of product}}{\text{Peak area between } 2\theta = 21.5\text{–}25.5^\circ \text{ of the most crystalline sample of the present study}}$$

Particle sizes were determined by scanning electron microscopy (JEOL JSM 5200). The products were further analyzed by IR (Perkin Elmer 221), ESR (Bruker E-2000), magnetic susceptibility, ion exchange capacity, and adsorption measurements. The oxidation reaction (*n*-hexane with H_2O_2) was carried out in a batch system. The products were analyzed by GC (HP 5880, capillary column, 50 m × 0.2 mm). The acid catalyzed reactions (such as *m*-xylene isomerization (21, 22) and ethylbenzene disproportionation (23, 24)) were carried out using a down-flow vertical silica (10 mm i.d., 30 cm long) reactor and the products were analyzed by on-line G.C using 5% bentone + 5% DIDP column.

RESULTS AND DISCUSSION

Synthesis

For the better incorporation of Ti and Fe in framework positions, the formation of TiO_2 and Fe_2O_3 should be avoided during the synthesis. The addition of ferric nitrate solution to the titanium silicate mixture, as in the case of [Al, Ti]–MEL, results in the formation of $Fe(OH)_3$ and eventually Fe_2O_3. To avoid the formation of $Fe(OH)_3$, a different procedure (given in the experimental section) was adopted for [Fe, Ti]–MEL: to ferric nitrate solution was added TEOS followed by TBOT and the template.

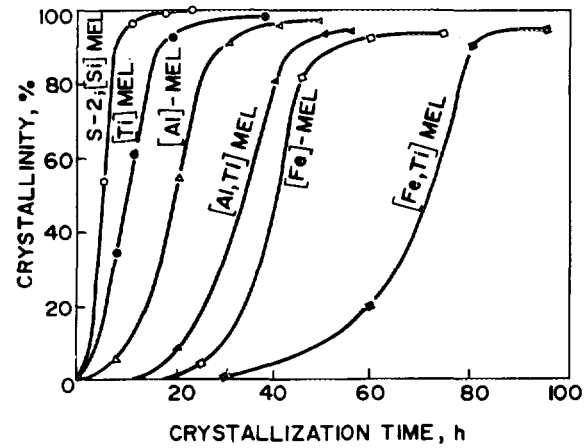

FIG. 1. Influence of the heterometal ion on the crystallization of metallo and metallo–titanium silicates.

The yield of all solid products (on SiO_2 basis) ranged between 85% and 95%. The influence of the nature of the heterometal ion on the rate of crystallization of metallo- and metallo–titanium silicates is shown in Fig. 1. The Al/Fe silicates crystallized faster compared to their respective metallo–titanium-silicate analogs. It is known that the incorporation of Al in high silica zeolites (such as MFI, MEL, MTT, MTW, etc.) is a slow process (25–27). This phenomenon seems to be valid for Fe^{3+} and Ti^{4+} also. Further, aluminosilicate molecular sieves crystallize faster than their corresponding [Fe]-analogs (5, 28).

Characterization

The X-ray powder diffraction pattern of silicalite-2 ([Si]–MEL), [Ti]–MEL, [Fe, Ti]–MEL, and [Al, Ti]–MEL (Fig. 2) confirmed their MEL structure (29). The absence of reflections at $2\theta = 9.05°$ and 24.05° and the presence of a doublet at 44°–45° (characteristic for MFI

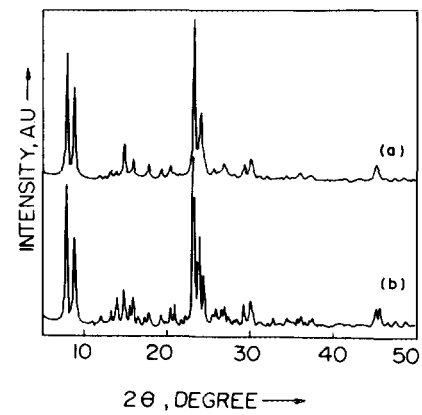

FIG. 2. X-ray diffraction patterns of (a) [Al]–MEL and (b) [Al]–MFI. The samples were calcined at 823 K in flowing air.

TABLE 1

Molar Composition and Unit Cell Parameters of [Si]-MEL, [Ti]-MEL, Metallo Silicates and Metallo-Titanium Silicates

Catalyst	Molar composition			Unit cell parameters[a]		
	Si/Ti	Si/Al	Si/Fe	$a = b$ (Å)	c (Å)	v (Å)^3
[Si]-MEL	—	>4000	—	20.046	13.391	5381.1
[Ti]-MEL	85	—	—	20.069	13.420	5405.1
[Al]-MEL	—	36	—	20.052	13.432	5400.9
[Fe]-MEL	—	—	40	20.102	13.460	5439.1
[Al, Ti]-MEL	92	30	—	20.094	13.427	5421.4
[Fe, Ti]-MEL	90	—	33	20.137	13.459	5457.6

[a] Calcined and hydrated before the measurements.

structure (30), Fig. 2(b)), in the XRD patterns of [*M*]-MEL and [*M*, Ti]-MEL samples confirms the absence of the corresponding MFI analogs.

The molar composition and unit cell parameters of [*M*]-MEL, [*M*, Ti]-MEL (*M* = Al or Fe), [Ti]-MEL, and silicalite-2 ([Si]-MEL) are reported in Table 1. The expansion in the unit cell follows the order [Si]- < [Al]- < [Ti]- < [Al, Ti]- < [Fe]- < [Fe, Ti]-MEL. The increase in the unit cell parameters of [*M*, Ti]-MEL as compared to silicalite-2 ([Si]-MEL) and [Ti]-MEL may be due to the presence of Ti^{4+} and Al^{3+}/Fe^{3+} ions in the silicalite framework.

Metallo-titanium silicates exhibit an IR band at 960 cm^{-1}, characteristic of the stretching mode of a [SiO_4] unit bonded (as (O_3Si-O-Ti)) to a Ti^{4+} ion (8, 18, 31) or a titanyl group (>Ti = O) (32, 33), strongly suggesting the presence of Ti^{4+} ions in the tetrahedral zeolite framework in our samples. This band was not observed either in the IR spectra of silicalite or in metallosilicates. Forni and Pelozzi (16) have also observed this band in [Al, Ti]-MFI.

The values of Mössbauer isomershift (δ) (at 298 K) exhibited by the white colored, calcined (at 753 K), and rehydrated (at 298 K) samples of [Fe]-MEL (34) and [Fe, Ti]-MEL were 0.27 mm/s and 0.25 mm/s, respectively, characteristic of the presence of Fe^{3+} ions in tetrahedral environment (4, 5). The magnetic moment values of calcined [Fe]-MEL were 5.8 and 5.7 Bohr magnetons. The corresponding values for [Fe, Ti]-MEL were 5.8 and 5.6 Bohr magnetons, indicating the presence of isolated Fe^{3+} ions with insignificant Fe-O-Fe type interactions (4, 5). The calcined [Fe]-MEL and [Fe, Ti]-MEL exhibited ESR signals at $g \sim 4.3$ and $g \sim 2.0$ due to distorted and undistorted symmetry of iron (III), in agreement with earlier observations on ferrisilicate zeolites (5, 34–38). However, an unambiguous assignment of ESR signals has been doubted recently (5, 37, 38). Ion-exchange and adsorption capacities of metallo and metallo-titanium silicates are reported in Table 2. The higher ion-exchange capacities of these materials can be taken as direct evidence for the presence of the trivalent metal ions in the framework, as they originate from the MO_2^- groups present in the tetrahedral position of the molecular sieve framework. Titanium silicate molecular sieves do not have any ion-exchange capacity. The adsorption capacities (Table 2) of all samples studied here were comparable to those reported in the literature (10) for MEL zeotypes, indicating the absence of any significant amount of occluded material within the zeolite channels. SEM photographs of [Al]-MEL, [Al, Ti]-MEL, [Fe]-MEL, and [Fe, Ti]-MEL are given in Fig. 3. The particle sizes of all these materials ranged between 0.5 and 1.5 μm.

Catalytic Properties

Table 3 shows the catalytic activity and selectivity of [Si]-MEL, [Ti]-MEL, [Al]-MEL, and [Al, Ti]-MEL in the oxyfunctionalization of *n*-hexane. As expected, [Ti]-MEL is the most active catalyst in the oxidation of *n*-hexane. When Ti is present in the lattice, hydrogen peroxide is selectively utilized for the oxidation reaction (7–10). The catalytic activity decreases in the order [Ti]- > [*M*, Ti]- > [*M*]- ~ [Si]-MEL. Brønsted acid

TABLE 2

Ion-Exchange and Adsorption Capacities of Metallo and Metallo-Titanium Silicates

Catalyst	Adsorption, wt%[a]		Ion-exchange capacity (K^+/MO_2^-)
	n-Hexane	Cyclohexane	
[Al]-MEL	12.4	6.9	0.90
[Fe]-MEL	12.3	6.2	0.84
[Al, Ti]-MEL	12.7	8.2	0.91
[Fe, Ti]-MEL	12.8	7.5	0.87

[a] $p/p_0 = 0.5$; T (K) = 298; after 2 h.

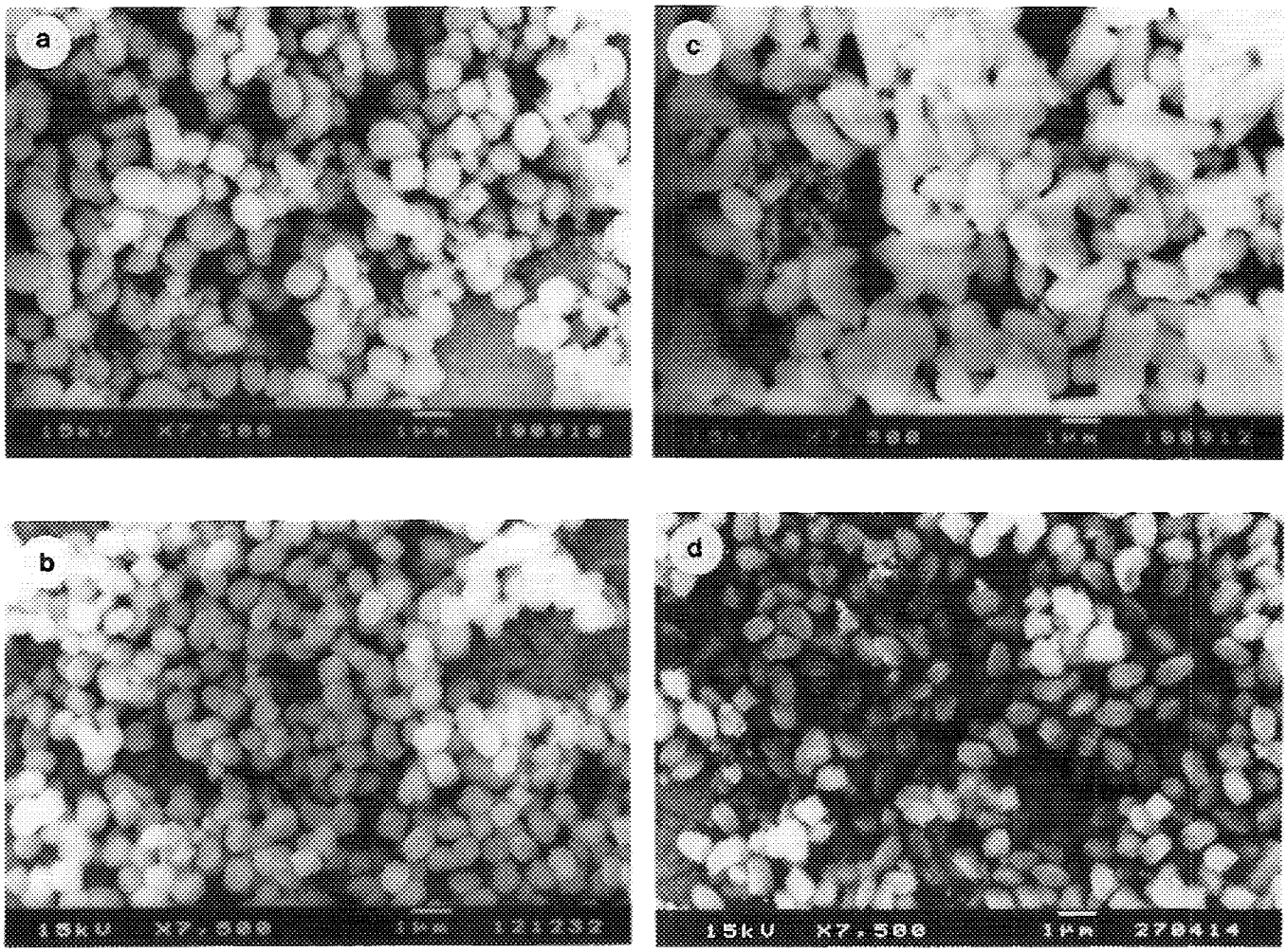

FIG. 3. Scanning electron micrograph of (a) [Al]–MEL, (b) [Al, Ti]–MEL, (c) [Fe]–MEL, and (d) [Fe, Ti]–MEL.

sites in metallosilicate analogs ([Al or Fe]–MEL) decompose the hydrogen peroxide, leading to lower H_2O_2 selectivity. This was confirmed by the higher activity of nonacidic Na–[Al, Ti]–MEL in n-C_6 oxidation than of acidic H–[Al, Ti]–MEL (Table 3).

Figure 4 compares the catalytic activity of [Al]– and [Al, Ti]– (Fig. 4(A)) and [Fe]– and [Fe, Ti]–MEL (Fig. 4(B)) in the isomerization of m-xylene as a function of time-on-stream. [Al]–MEL deactivated faster than [Al, Ti]–MEL. The former also has a higher paraselectivity (p-/o-ratio) than the latter (Fig. 5). On the other hand, both [Fe]–MEL and [Fe, Ti]–MEL possess similar deactivation and shape-selective characteristics. Since the crystal size and shape of all the MEL samples studied here are comparable (Fig. 3), the lower para selectivity of [Al, Ti]–, [Fe]–, and [Fe, Ti]–MEL vis-à-vis the strongly acidic [Al]–MEL indicates the important role of the strength of acid sites in controlling product shape-selectivity. This is more clearly illustrated in Fig. 6, where the value of the p-/o-ratio is plotted against m-xylene conver-

TABLE 3

Oxidation of n-Hexane over Different MEL Molecular Sieves

Catalyst	n-C_6 conversion (wt. %)	H_2O_2[a] utilization (mole %)	2–/3– ratio[b]	Product selectivity[c]
[Ti]–MEL	11.3	33.0	1.2	85.5
H–[Al, Ti]–MEL	7.8	12.0	1.3	61.1
Na–[Al, Ti]–MEL[d]	10.1	18.6	1.2	66.9
H–[Al]–MEL	5.3	4.9	1.5	36.5
[Si]–MEL	3.3	3.1	1.2	27.1

Note. T (K) = 373; 0.58 moles n-C_6/g catalyst; n-C_6 : H_2O_2 = 3 : 1; solvent = acetone (20 ml); reaction time = 5 h.

[a] H_2O_2 utilized for oxy-functional product formation.

[b] The 2–/3–ratio = (2-hexanol + 2-hexanone/3-hexanol + 3-hexanone).

[c] Product selectivity = (Σ2– and 3– compounds/n-hexane reacted) × 100.

[d] H–[Al, Ti]–MEL is refluxed twice in 1 N sodium sulfate for 1 h and calcined at 773 K to obtain Na–[Al, Ti]–MEL. The Na/Al ratio in the resultant sample is 1.0.

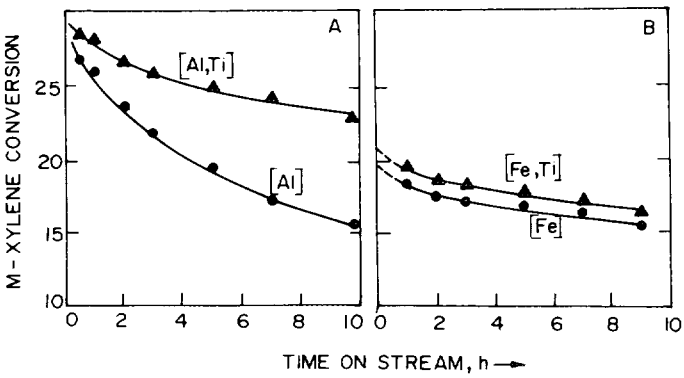

FIG. 4. *m*-xylene isomerization over MEL type metallosilicates. *T* (K) = 553; Pressure = 1 atm; LHSV (h^{-1}) = 4; H_2/*m*-xylene (mole) = 4.

sion. The difference in *p*-/*o*-ratio becomes less significant at higher *m*-xylene conversions (>30%), i.e., near to the equilibrium conversions. However, the difference in *p*-/*o*-ratio is clearly seen over a broad range of *m*-xylene conversions (5–35%). In the alkylation of toluene with methanol, Corma (39) has also reported that the para-selectivity increases with the strength of the Brønsted acid sites. On weakly acidic catalysts the overall rate is probably controlled by the chemical reaction step. On strongly acidic catalysts, on the other hand, transport processes constitute the slow rate determining step and, hence, differences in the relative diffusivities of the various product molecules lead to the observed product shape-selectivity phenomenon.

CONCLUSIONS

(1) We have incorporated Ti^{4+} as well as Al^{3+}/Fe^{3+} into the MEL (silicalite-2) framework.

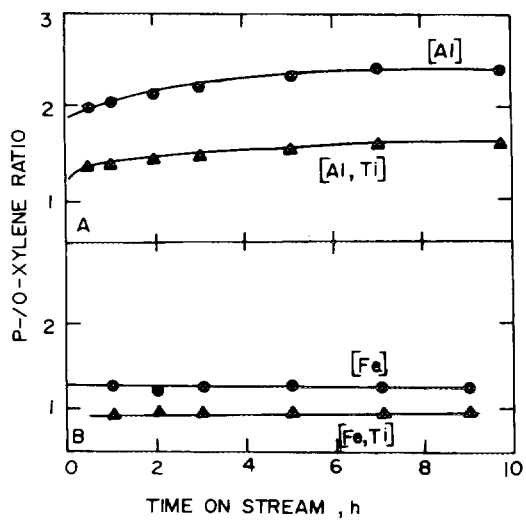

FIG. 5. *p*-/*o*-xylene ratios over MEL type metallosilicates. *T* (K) = 553; Pressure = 1 atm; LHSV (h^{-1}) = 4; H_2/*m*-xylene (mole) = 4.

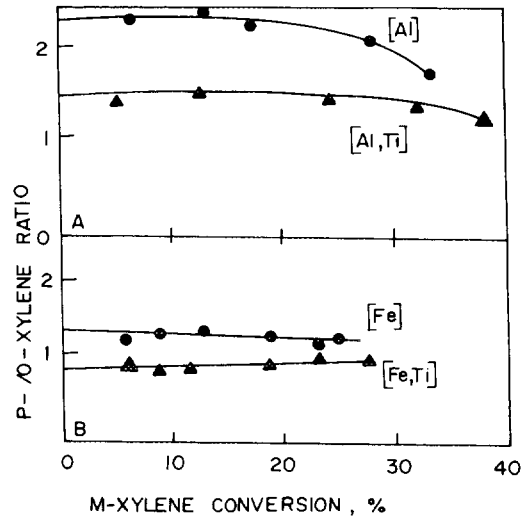

FIG. 6. Effect of conversion level on the *p*-/*o*-xylene ratio over MEL type metallo silicates. Pressure = 1 atm; LHSV (h^{-1}) = 4; H_2/*m*-xylene (mole) = 4; *T* is varied to get different conversions.

(2) Our MEL type metallo-titanium silicates do not contain any detectable amount (by XRD) of MFI impurities.

(3) An expansion in the unit cell parameters (XRD), the occurrence of the 960 cm^{-1} band in the framework IR spectra, Mössbauer I.S. (δ = 0.25–0.27 mm/s), magnetic susceptibility (μ = 5.6–5.8 Bohr magneton), and high ion-exchange capacities (K^+/MO_2^-) = 0.84-0.91, *M* = Al or Fe) observed in our samples strongly suggest that these metal ions are incorporated in the MEL framework.

(4) The metallo-titanium silicate analogs crystallize at a slower rate than corresponding metallo silicates.

(5) Metallo-titanium silicates exhibit catalytic activity in both acid-base and oxidation catalytic reactions.

(6) H-[Al, Ti]-MEL, H-[Fe, Ti]-MEL, and H-[Fe]-MEL are less para-selective vis-à-vis H-[Al]-MEL.

(7) In Brønsted acid catalyzed reactions metallo-titanium silicates deactivate at a slower rate than the metallo silicate analogs.

ACKNOWLEDGMENTS

JSR thanks CSIR for a research fellowship. We thank Dr. Paul Ratnasamy for his valuable suggestions and for reviewing the manuscript. We also thank K. Ramesh Reddy and Anuj Raj for their help during the study. This work was partly funded by UNDP.

REFERENCES

1. Barrer, R. M., Baynam, J. W., Bultitride, F. W. and Meier, W. M., *J. Chem. Soc.* **195** (1959).
2. Breck, D. W., "Zeolite Molecular Sieves: Structure, Chemistry and Uses," p. 320. Wiley Interscience, New York, 1974.
3. Barrer, R. M., "Hydrothermal Chemistry of Zeolites." Academic Press, New York, 1982.

4. Szostak, R., "Molecular Sieves: Principles of Synthesis and Identification." Van Nostrand–Reinhold, New York, 1989.
5. Ratnasamy, P., and Kumar, R., "Ferrisilicate Analogs of Zeolites." *Catal. Today* **9** (4) (1991).
6. Young, D. A., U.S. Patent 3,329,480. 1967.
7. Taramasso, M., Perego, G., and Notari, B., U.S. Patent 4,578,521. 1983.
8. Notari, B., *Stud. Surf. Sci. Catal.* **37,** 413 (1988); Notari, B., *Stud. Surf. Sci. Catal.* **60,** 343 (1990).
9. Thangaraj, A., Kumar, R., Mirajkar, S. P., and Ratnasamy, P., *J. Catal.* **130,** 1 (1991).
10. Reddy, J. S., Kumar, R., and Ratnasamy, P., *Appl. Catal.* **58,** L1 (1990).
11. Reddy, J. S., and Kumar, R., *J. Catal.* **130,** 440 (1991).
12. Reddy, J. S., and Kumar, R., *Zeolites*, **12,** 95 (1992).
13. Reddy, J. S., Sivasanker, S., and Ratnasamy, P., *J. Mol. Catal.* **69,** (3), 383 (1991).
14. Reddy, J. S., Sivasanker, S., and Ratnasamy, P., *J. Mol. Catal.* **70** (3), 335 (1992).
15. Bellusi, G., EP Applied A1 0272496. 1987.
16. Forni, L., and Pelozzi, M., *J. Mater. Chem.*, 1101 (1990).
17. Thangaraj, A., Kumar, R., and Sivasanker, S., *Zeolites* **12,** 129 (1992); Thangaraj, A., Kumar, R., and Ratnasamy, P., *Appl. Catal.* **57,** L1 (1990).
18. Bellussi, G., Carati, A., Clerici, M. G., and Esposito, A., *Stud. Surf. Sci. Catal.* **63,** 421 (1991).
19. Reddy, J. S., and Kumar, R., in "Proc. 10th Natl. Symp. on Catal. and 4th Indo-USSR Symp. on Catal.," Recent Developments in Catalysis (B. Viswanathan *et al.*, Eds.), p. 156. Narora, New Delhi, 1989.
20. Camblor, M. A., Corma, A., Martinez, A., and Pérez-Pariente, J., *J. Chem. Soc. Chem. Commun.*, 589 (1992).
21. Dewing, J., *J. Mol. Catal.* **27,** 25 (1984).
22. Martens, J. A., Perez-Pariente, J., Sastre, E., Corma, A., and Jacobs, P. A., *Appl. Catal.* **45,** 85 (1988).
23. Karge, H. G., Hatada, J., Zang, Y., and Fiedorow, R., *Zeolites* **3,** 13 (1983).
24. Weitkamp, J., Ernst, S., Jacobs, P. A., and Karge, H. G., *Erdöl Kohle Erdgas Petrochem.* **39,** 13 (1986).
25. Rammanikov, V. N., Mastikhin, V. M., Hocevar, S., and Drzaj, B., *Zeolites* **3,** 311 (1983).
26. Ernst, S., Jacobs, P. A., Martens, J. A., and Weitkamp, J., *Zeolites* **7,** 458 (1987).
27. Ernst, S., Kumar, R., and Weitkamp, J., *in* "Zeolite Synthesis" (M. L. Occelli and H. E. Robson, Eds.) ACS Symposium Series No. 398, p. 560. Amer. Chem. Soc., Washington, DC, 1989.
28. Ball, W. J., Dwyer, J., Garforth, A. A., and Smith, W. J., *in* "New Developments in Zeolite Science and Technology" (Y. Murakami *et al.*, Eds.), *Studies in Surface Science Catalysis*, Vol. 28, p. 137. Elsevier, Amsterdam, 1986.
29. Kokotailo, G. T., Chu, P., Lawton, S. L., and Meier, W. M., *Nature* **275,** 119 (1978).
30. Kokotailo, G. T., Lawton, S. L., Olson, D. H., and Meier, W. M., *Nature* **272,** 437 (1978).
31. Boccuti, M. R., Rao, K. M., Zecchina, A., Leofanti, G., and Petrini, G., *in* "Structure and Reactivity of Surfaces" (C. Morter *et al.*, Eds.), *Studies in Surface Science and Catalysis*, Vol. 48, p. 133. Elsevier, Amsterdam, 1989.
32. Perego, G., Bellussi, G., Corno, C., Taramasso, M., Buonomo, F., and Esposito, A., *Stud. Surf. Sci. Catal.* **28,** 129 (1986).
33. Huybrechts, D. R. C., Bruycker, L. D., and Jacobs, P. A., *Nature* **345,** 240 (1990).
34. Reddy, J. S., Reddy, K. R., Kumar, R., and Ratnasamy, P., *Zeolites* **11,** 553 (1991).
35. Handreck, G. P., and Smith, T. D., *J. Chem. Soc. Faraday Trans. I* **85,** 319 (1989).
36. Kumar, R., and Ratnasamy, P., *J. Catal.* **121,** 89 (1990).
37. Lin, D., Ph.D., Thesis No. 126-89. University of Clande, Birnard, Lyon, France, 1989.
38. Patarin, J., Ph.D. Thesis. University of Mullhouse, France, 1988.
39. Corma, A., *in* "Guidelines for Mastering the Properties of Molecular Sieves" (D. Barthomeuf *et al.*, Eds.), NATO ASI Series, Series B: Physics, Vol. 221. Plenum, New York, 1990.